

# Experimental Design Supported Formulation and Evaluation of Nanostructured Lipid Carrier Loaded Oro mucosal Film of Tenofovir Disoproxil Fumarate

Kavitha HK <sup>1</sup> , Sayani BHATTACHARYYA <sup>2\*</sup> 

<sup>1</sup> Department of Pharmaceutics, Krupanidhi College of Pharmacy, Bangalore, 560035, Karnataka India

\* Corresponding Author. E-mail: sayanibh@gmail.com (N.S.); Tel. +91-984-5561865.

Received: 18 April 2023 / Revised: 06 July 2023 / Accepted: 03 August 2023

**ABSTRACT:** Antiretroviral medication tenofovir disoproxil fumarate (TDF) is frequently used to treat HIV and Hepatitis B virus infection and possesses low oral bioavailability due to low cellular penetration, and intestinal degradation. The present research focuses to develop nanoparticle-loaded oral film of TDF for the pediatric population with an aim to improve bioavailability and patient compliance. A high-shear homogenization process was employed to prepare nanostructured lipid carriers (NLCs) of TDF using an I-Optimal design. The consequences of proportions of solid and liquid lipid, and surfactant concentrations on drug entrapment, loading, and particle size were studied with a planned 14 experimental runs. The optimized formulation was loaded into an oromucosal film using hydroxy propyl methyl cellulose (HPMC) polymer. The films were evaluated for their physicochemical, and mechanical properties. The permeation of the drug from the films through goat oral mucosa was estimated. The design yielded an optimized product characterized by its nanosized (215 nm), stability (0.1 mV), and high entrapment (95.6%) of TDF in the carrier matrix. The surface morphology proved the irregular surface of the nano lipid carrier. The oro-mucosal film exhibited prolonged residence time and was released gradually over 24 h. The permeation of the drug from the nanocarriers loaded film was significantly improved compared to the pure drug. These findings support the idea that NLC-loaded oro-mucosal adhesive films may represent a promising strategy for increasing TDF's oral bioavailability.

**KEYWORDS:** Tenofovir Disoproxil Fumarate; Nano lipid carriers; High shear homogenization; Oro mucosal adhesive film; Solvent Casting method.

## 1. INTRODUCTION

Tenofovir disoproxil fumarate (TDF) is an antiretroviral drug that is widely used in the treatment of infection caused by HIV, HBV, and Herpes simplex virus-2[1]. TDF belongs to BCS class III and possesses low oral bioavailability and low cellular penetration due to intestinal degradation and efflux transport. Currently, TDF is available in the form of tablets for oral use for adults and as a powder for the pediatric population. The absorption of drugs from oral administration is highly affected by the type of food intake. A novel delivery of the drug to overcome the limitations of oral administration, and easy delivery for all age groups could be beneficial to improve the therapeutic efficacy of TDF. Hence a nano-lipid carrier loaded oro-mucoadhesive film is proposed for the present study. Nanostructured lipid carriers (NLCs) represent the second generation of lipid nanoparticles consisting of mixtures of solid and liquid lipids with emulsifiers. Liquid lipid generates structural flaws in the solid lipids that change their crystalline structure and makes it easier for lipophilic or hydrophilic medicines to bind to the matrix.[2]. The employment of physiological lipid materials as components for NLCs offers compatibility, improved bioavailability, and biodegradability[3]. NLCs are explored for the controlled and targeted delivery of drugs through parenteral, topical, and oral routes[3-4].

The oro-mucosal drug delivery offers the advantages of ease of administration, improved bioavailability, and patient compliance. The oro mucosal delivery can be used for prolonged oral delivery of drugs directly to the systemic circulation bypassing the detrimental effect of oral administration[5]. Though the buccal mucosa offers less absorptive surface area, the high vasculature, presence of lymphatic circulations, and less enzymatic activity helps in better drug absorption. Furthermore, mucoadhesive oral delivery through adhesive films offers the advantages of overcoming uncontrolled swallowing, saliva flush, and removal from the site on ingestion of food[6]. The oromucosal adhesive films are anticipated to have a longer residence time and can be tailored to control hydration and swelling. Hence the present study proposes a mucoadhesive

HK Kavitha, Bhattacharyya S. Experimental Design Supported Formulation and Evaluation of Nanostructured Lipid Carrier Loaded Oromucosal Film of Tenofovir Disoproxil Fumarate, J Res Pharm. 2024; 28(4): 940-951.

buccal film for TDF in nano lipid carriers. The permeation of the drug can be improved with the nanocarriers. The mucoadhesive film so designed can sustain the release of the drug directly in the systemic circulation bypassing efflux transport and food effects in the intestine [7]. Hence, the proposed nanocarrier-loaded mucoadhesive buccal film can be applicable for a planned patient-focused delivery for better and novel treatment. This can improve patient's quality of life and reduce the chances of nonadherence to chronic treatment. Hence the oral film might serve as a promising delivery of TDF.

## 2. RESULTS AND DISCUSSION

### 2.1. Solubility of the drug in lipids

The larger loading capacity and drug entrapment efficiency of the drug in the lipid matrix are approximately estimated by the solubility of the drug in the solid and liquid lipid phases. The drug exhibited high solubility in stearic acid and oleic acid as reported in **Hata! Başvuru kaynağı bulunamadı.** and **Hata! Başvuru kaynağı bulunamadı.** In order to prepare the NLC of TDF, stearic acid and oleic acid were chosen as the solid and liquid lipids, respectively.

**Table 1.** Selection of solid lipids.

Name of the solid lipid	Drug quantity (mg) dissolved in a fixed quantity of lipid	Observation
Stearic acid	25±1.05	Obscure
Beeswax	15±0.90	Obscure to hazy
Glyceryl Behenate	15±1.16	cloudy

\*All the values are mean of triplicate ± SD.

**Table 2.** Selection of liquid lipids.

Oil	Solubility (mg/ml)
Olive oil	34.478±0.53
Oleic acid	53.09±0.49
Castor oil	40.162±0.61

\*All the values are mean of triplicate ± SD.

### 2.2. Evaluation and optimization of design

Optimal designs are computationally intensive with a set of users' specified points. The accommodation of critical component factors in I-optimal design was naturally applied to predict the variance over a region of the parameter value. The design yielded 14 experimental runs, and an overview of the outcome is presented in **Hata! Başvuru kaynağı bulunamadı.**

The ANOVA analysis clearly indicated that the lipid ratio (SL: LL) had a remarkable effect on drug entrapment and particle size, whereas drug loading was significantly affected by the confounding effect of lipid ratio and concentration of surfactant. The influences of the factors on the responses were further studied with 2D contour plots and 3D response surface plots (**Hata! Başvuru kaynağı bulunamadı.**).

The contour plot of entrapment efficiency depicted the nonlinear increment in entrapment of TDF with the increase of lipid ratio and surfactant concentration, whereas the response surface plot revealed the significant effect of lipid ratio on the entrapment. The contour plot of drug loading elucidated the nonlinear decrease in drug loading with the increase in lipid ratio. However, the response surface diagram of the same showed a flattening of the graph toward lipid ratio and surfactant concentration and revealed the combined effect of both factors on the drug loading in the NLC matrix. A linear relation of factors on particle size was revealed from the contour plot of particle size. An increase in lipid ratio increased the particle size. A greater curvature towards the lipid ratio in the response surface diagram of particle size illustrated the fact that the lipid ratio has a stronger influence on particle size than the surfactant concentration in the preparation of NLC of TDF. The optimization of the design was attended at trading off of the responses at Entrapment efficiency  $\geq 90\%$ , drug loading  $\geq 35\%$ , and particle size  $\leq 200$  nm. The optimization yielded a desirability of 0.779 and suggested optimized formulation factors at a coded value of SL: LL= -0.09 and concentration of surfactant= 1. Model validation was carried out by experimenting at the optimized ratio and %bias was found to be less than 10% as Table 4. The measured responses for all the formulations were subjected to parameter sensitivity analysis using Design Expert software V11. The main and interactive factors resulted in model equations as projected in **Hata! Başvuru kaynağı bulunamadı.**

**Table 3.** Outcome of the experimentation of the I optimal design for the responses.

Formulation code	%Entrapment efficiency	% Drug loading	Particle Size (nm)
F1	98.892±0.025	47.822±0.008	145±31.2
F2	99.476±0.024	48.638±0.007	113±12.9
F3	98.116±0.031	44.590±0.010	223±20.4
F4	97.703±0.025	51.617±0.006	125±10.9
F5	96.757±0.009	25.739±0.014	136±14.8
F7	98.495±0.005	31.376±0.012	178±30.5
F8	98.808±0.014	30.884±0.001	219±16.7
F9	96.461±0.002	27.625±0.011	286±13.4
F10	98.574±0.036	53.485±0.006	134±12.3
F11	97.741±0.017	38.440±0.004	162±8.9
F12	98.653±0.004	49.120±0.010	321±21.6
F13	97.377±0.001	45.453±0.010	236±17.8
F14	97.288±0.028	26.959±0.003	267±15.1

\*All the values are mean of triplicate ± SD

**Table 4.** Predicted vs. experimented results of the optimized formulation.

Response	Predicted	Experimented	% Bias
%Entrapment efficiency	97.909	95.76±0.5	2.19
% Drug loading	38.34	36.19±0.08	5.60
Particle Size (nm)	207	215.6±12.48	4.15

\*All the values are mean of triplicate ± SD.

**Table 5.** Model and parameter sensitivity statistics through ANOVA.

Response	Source	P-value	Effect	Model Equation
% Entrapment efficiency	A-SL: LL	0.0074	Significant	Sqrt (R1) =
	B- Conc of surfactant	0.0036	Significant	+9.76072
	AB	0.0123	Significant	-0.154099 A
	B <sup>2</sup>	0.0123	Significant	+0.651082 B
	B <sup>3</sup>	0.0033	Significant	+0.203273 A <sup>2</sup> * B <sup>2</sup> +0.243429 B <sup>2</sup> -0.756654 B <sup>3</sup>
% Drug loading	A-SL: LL	0.0531		R2 =
	B-Conc of surfactant	0.7974		+37.82671 -7.69256 A
	AB	0.0259	Significant	+0.939340 B
				+12.52058 A <sup>2</sup> * B <sup>2</sup>
Particle Size (nm)	A-SL: LL	0.0003	Significant	R3 =
	B-Conc of surfactant	0.6662		+206.90591 +77.43593 A +6.72592 B

\*A= SL: LL B= Concentration of surfactant

\*All the values are mean of triplicate ± SD.

### 2.3. Estimation of particle size and zeta potential

Dynamic light scattering method was used employed to determine the particle size of the optimized product. The formulated NLC had a particle size and zeta potential of 215.6 nm and 0.1mV respectively. The negative surface charge of the molecule limits the penetration of the drug through the biological membrane as reported[8]. Hence, the entrapment of the drug in the carrier with a positive charge might influence its permeation and absorption. The optimized formulation showed a positive surface charge of 0.1 mV which might contribute enhancement of the permeability of TDF.

### 2.4. Fourier Transform Infrared (FTIR) Spectroscopy

The molecular structures of the blank and optimized NLC formulation were clarified using ATR-FTIR, focusing special emphasis on the interactions between the drug and the excipients. The spectrum of TDF showed NH<sub>2</sub> stretching vibrations at 3322 cm<sup>-1</sup>, OH bands at 3200 cm<sup>-1</sup> and 3300 cm<sup>-1</sup>, CH aliphatic stretching out of plane CH<sub>2</sub> and CH bending at 2980 cm<sup>-1</sup>, 724 cm<sup>-1</sup> and 654 cm<sup>-1</sup> respectively. CH<sub>2</sub> asymmetric stretching

at 2980  $\text{cm}^{-1}$ , C=O stretching at 1752  $\text{cm}^{-1}$ , P stretch at 1673  $\text{cm}^{-1}$ , medium stretch  $\text{NH}_2$  scissoring at 1557  $\text{cm}^{-1}$  and 1580  $\text{cm}^{-1}$ , aromatic C=N stretch in pairs at 1421  $\text{cm}^{-1}$  and 1444  $\text{cm}^{-1}$ , symmetric aliphatic CH bending of  $\text{CH}_3$  at 1376  $\text{cm}^{-1}$ , C-O stretch at 1256  $\text{cm}^{-1}$ , C=C stretching in the aromatic ring at 1256  $\text{cm}^{-1}$ , medium stretch C-N deformation at 1256  $\text{cm}^{-1}$ , aliphatic ether stretch vibration 1095  $\text{cm}^{-1}$  and 1138  $\text{cm}^{-1}$ , C-O group/ $\text{CH}_2\text{OH}$  stretching at 1138  $\text{cm}^{-1}$  and 1095  $\text{cm}^{-1}$ , out of plane OH stretching at 951  $\text{cm}^{-1}$  and aromatic ring with plane bending at 695  $\text{cm}^{-1}$ . The same peaks of the drug were observed in the optimized formulation. The reduction in the intensity of C=N stretch and C=O stretch in the formulation indicated high entrapment of the drug in the formulation [9]. The characteristic peaks of the blank formulation at 2915  $\text{cm}^{-1}$ , 2848  $\text{cm}^{-1}$ , 1700  $\text{cm}^{-1}$ , 1453  $\text{cm}^{-1}$ , and 1099  $\text{cm}^{-1}$  were preserved in the optimized drug-loaded formulation. Hence, ATR-FTIR concludes that no interactions were observed between the drug and the excipients as presented in **Hata! Başvuru kaynağı bulunamadı.**

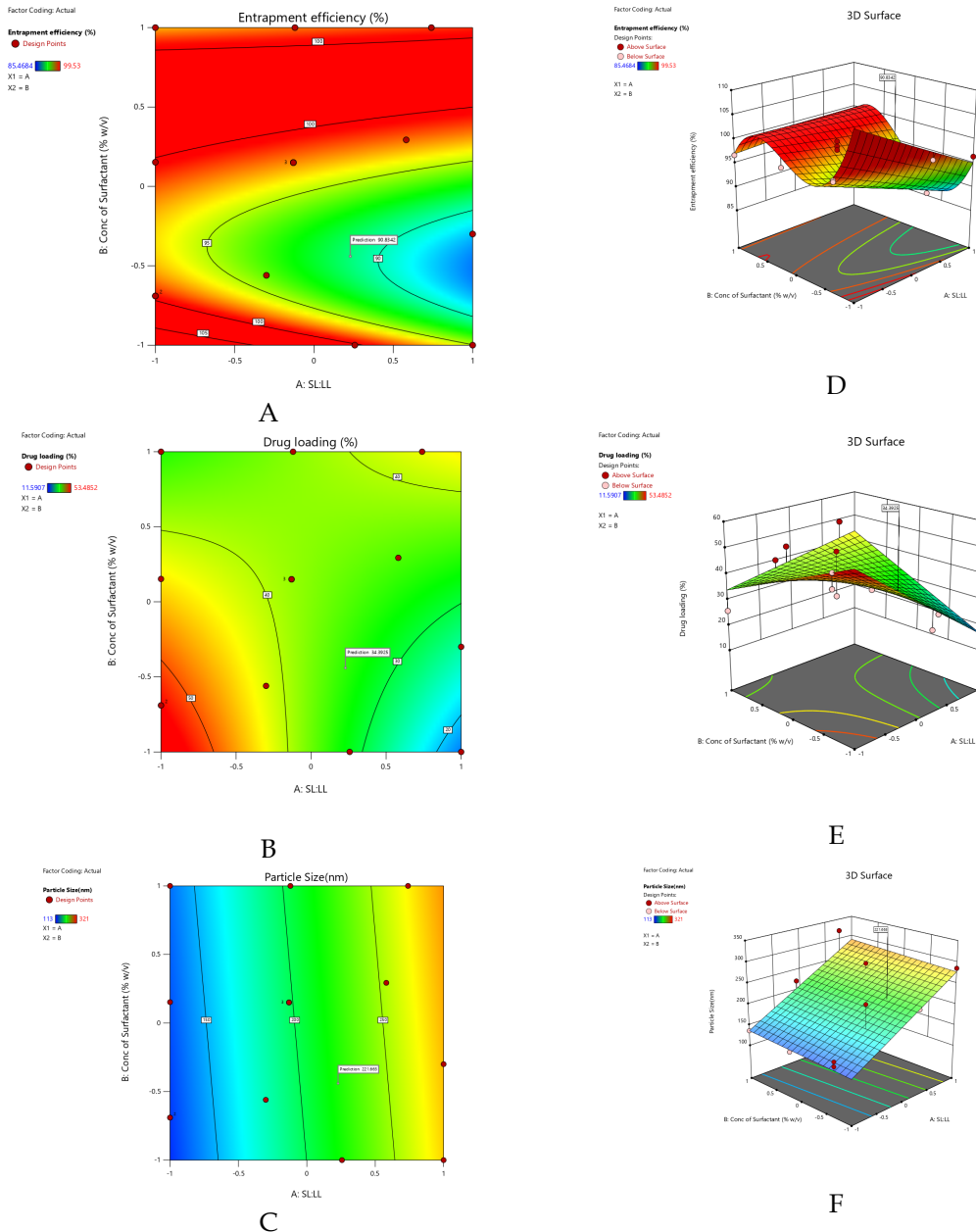


**Figure 1.** 2D Contour Plots of Entrapment efficiency(A), Drug loading(B), and Particle Size(C), and 3D Response surface plot for Entrapment efficiency(D), Drug loading(E), and Particle Size(F).

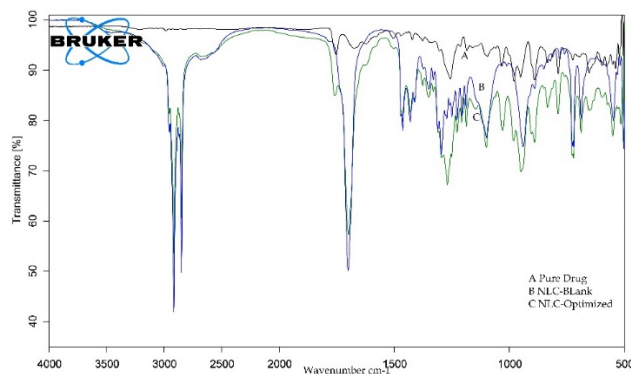


Figure 1. FTIR spectra of pure drug (A), blank NLC, and Optimized NLC (B).

FTIR study of the pure drug authenticates the identity of the drug. The spectrum of drug-loaded nano lipid carriers retained the major functional peaks of the drugs but with lesser intensities, which might be due to the formation of the H-bond, and represented no specific interaction between the drug and excipients.

### 2.5. Scanning Electron Microscopy (SEM)

Scanning electron microscopy (SEM) pictures (as shown in **Hata! Başvuru kaynağı bulunamadı.**) of the optimized formulation revealed the structure of the nanoparticles and the presence of irregular surfaces was detected. The micrograph revealed the nano size of the formulations and the presence of aggregation might be due to the untrapped lipid carrier.

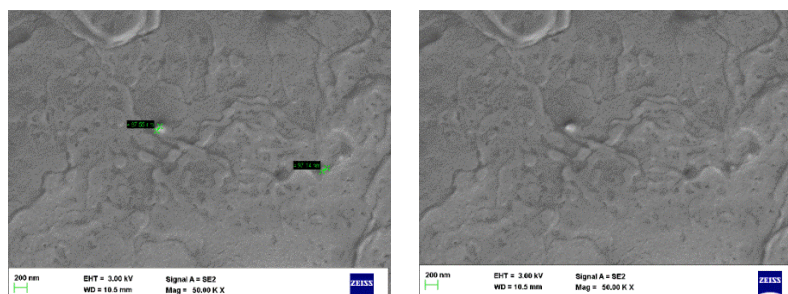


Figure 2. SEM of NLC of TDF.

### 2.6. In-vitro drug release study for NLC

The optimized nano lipid carriers showed the highest % cumulative drug release of 58.57% in 8h as represented in **Hata! Başvuru kaynağı bulunamadı.** The release of entrapped drug from the NLCs was found to be biphasic which is an indication of the imperfections in the structure. The initial release was around 19% followed by a sustained release of the drug. The initial burst release was due to the untrapped drug on the outer shell containing the liquid lipids, followed by matrix erosion that led to a sustained release over time[10].

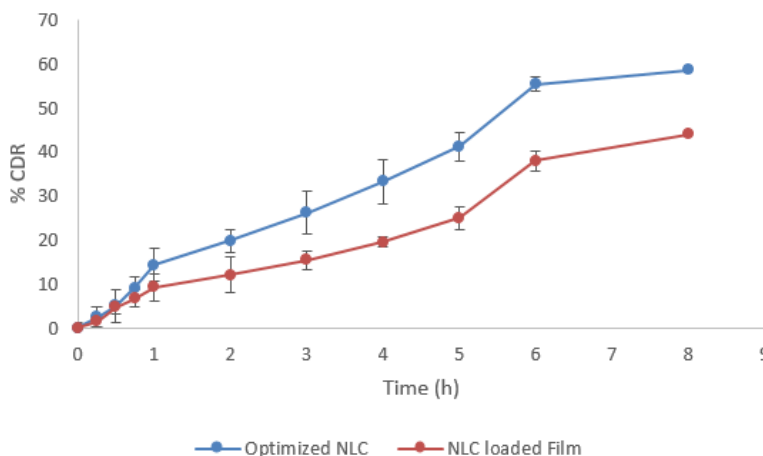


Figure 3. In vitro drug release study of optimized NLC.



The NLC-loaded film showed a slightly lower release but showed the same pattern of biphasic release. The in vitro release of the drug follows first-order kinetics. In both cases, the Korsmeyer Peppas exponent was found to be  $> 1$  in the initial phases of drug release, which proved anomalous release and constituted the reason for the burst release. In the later phase, the Korsmeyer Peppas exponent was found to be  $< 0.8$ , which indicated case-II matrix release due to erosion and resulted in the gradual release of the drug.

## 2.7. Evaluation of oro-mucosal adhesive films of TDF

### 2.7.1. Muco-adhesion property

Muco-adhesion time of NLC-loaded oro-mucosal adhesive film was found to be  $24 \pm 0.23$ h, which predicted the maximum residence and adhesion time of the film in oral hygiene.

### 2.7.2. Mechanical properties of the film

The prepared film has a thickness of  $11 \pm 0.50$  cm, and the folding endurance was found to be  $20 \pm 1$ . The thickness and folding endurance ensured that the film has sufficient elasticity and resistance to puncture, hence can be suitable for administration, without breaking [11]. The presence of HPMC and Carbopol 934 together might have contributed to the elasticity of the film to resist puncture.

### 2.7.3. Surface pH test

The pH of the film was found to be 6.9 which is suitable for oral administration of the film. The oral mucosa is having a pH of 6.8, and the optimized NLC-loaded film showed a surface pH of 6.9 which is near to the pH of the oral mucosa, hence oral irritation can be avoided.

### 2.7.4. Swelling test

The swelling behaviour of the NLC-loaded film was found to be  $< 10$  % which depicted that the film would retain its adhesion property and also patient compliance.

### 2.7.5. Content uniformity

The content uniformity of the film showed that  $23.08 \pm 0.05$  mg of TDF was present in the  $4 \text{ cm}^2$  area of the film.

### 2.7.6. Differential Scanning Calorimetry (DSC)

The endothermic peak of the pure drug which corresponds to its melting point was seen at  $113^\circ\text{C}$ . The thermogram of the optimized formulation revealed no drug peak, indicating that the drug was dispersed throughout the lipid matrix. This is a sign that the drug is highly entrapped in the lipids. The absence of drug peak in the mucoadhesive film of the optimized formulation revealed uniform dispersion of the NLC in the HPMC film **Hata! Başvuru kaynağı bulunamadı..**

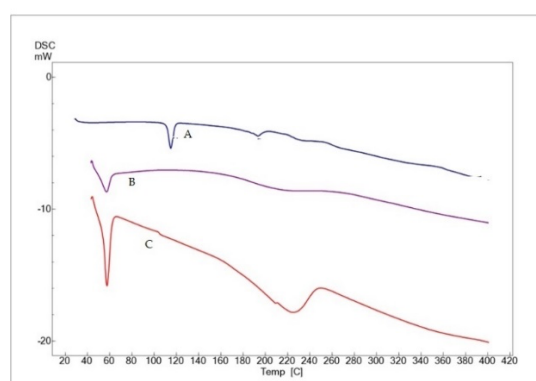


**Figure 4.** DSC thermograms of the pure drug (A), Optimized NLC (B), and NLC-loaded film (C).

The broadened peak at  $220^\circ\text{C}$  on the thermogram of the film corresponds to the polymer mixture[12]. This is an indication of the miscibility of the formulation in the polymer. The glass transition temperature of the film was greater than the temperature of the buccal cavity and proves the stability of the film during manufacture and storage.

### 2.7.7. Ex-vivo permeation study

**Hata! Başvuru kaynağı bulunamadı.** displays the result of the *ex-vivo* permeation study. The NLC-loaded oro-mucoadhesive film exhibited better permeability through goat oral mucosa compared to the film of pure drug. The NLC-loaded oral film showed a much higher *ex-vivo* release profile compared to the film of pure drug. The permeation parameters were enhanced remarkably. The drug flux and permeation were enhanced by 3.5 times as shown in **Hata! Başvuru kaynağı bulunamadı.**

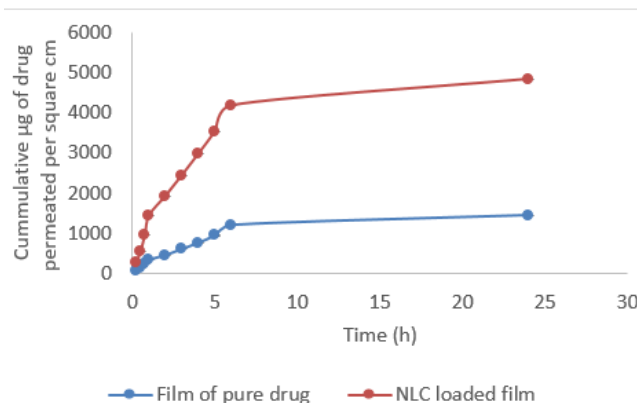


Figure 5. Ex vivo permeation study.

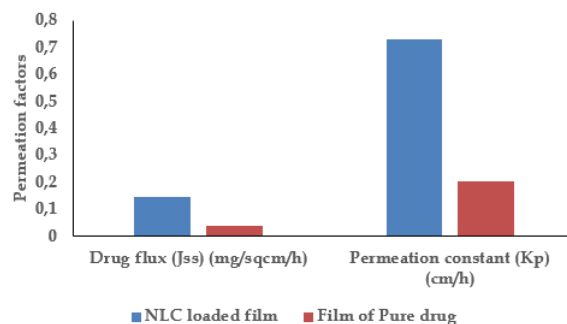


Figure 6. Estimation of permeation parameters.

## 3. CONCLUSION

Successful development of nano lipid carriers loaded film of TDF can be an optimistic way to provide systemic action of TDF for the pediatrics which overcomes the challenges of low oral bioavailability due to lesser cellular penetration and efflux transport in the intestine. The challenges of entrapping hydrophilic drug in the lipid core were met with the application of robust experimental design. The nano lipid carriers showed high entrapment of the drug, and the positive surface charge of the particles showed the possibility of improved permeation. The drug release from the nanoparticles was found to be biphasic. The film of the nanocarriers of the drug exhibited good physicochemical and mechanical stability as an oral film, Its integrity was preserved for 24 h and demonstrated a sustained release of the drug. The drug permeation was enhanced significantly. Hence it can be concluded that the newly developed oromucosal film of TDF could overcome the limitations of poor permeation and exhibited stability in saliva, provided good mucoadhesion and adequate drug release for long hours.

## 4. MATERIALS AND METHODS

We received a gift sample of TDF from Viatrix, Hyderabad. Excipients such as oleic acid, olive oil, castor oil, beeswax, stearic acid, glyceryl behenate, poloxamer 188, Carbopol 934, HPMC, HPC.iso-propyl alcohol, dichloromethane, propylene glycol were obtained from SD fine chemicals, Mumbai.

### 4.1. Solubility determination of drug in lipids

Screening of lipids constitutes the primary step in the formulation of NLCs. This is because drug solubility in the lipid medium impacts the formulation's stability, entrapment effectiveness, and capacity for drug loading [13]. During the screening of solid lipids, a large amount of the drug was taken and mixed with

molten lipids in a China dish under a constant temperature of 70 °C in a water bath with constant stirring until it dissolves[14]. In the case of liquid lipid 1ml of oil was taken in an Eppendorf tube containing 1ml water, to this 10 mg of the drug was added, vortexed, and kept in a mechanical shaker for 24h. This mixture is further centrifuged for 15 min at 15000 rpm. From the supernatant layer, 0.1 ml was taken in a 10 ml volumetric flask, and volume was made with a mixture of 1:1 ratio of phosphate buffer (pH 2.5) and acetonitrile. The drug was estimated using UV spectrophotometer (UV Vis Spectrophotometer Tech comp 23.1 Shimadzu, Japan) at 250 nm using the linear equation  $Y = 0.0253X - 0.0155$  where Y- absorbance and X concentration.

#### 4.2. Identification of the critical factors and levels for NLC of TDF

A preformulation study was carried out to identify the formulation factors and their levels that are critically affecting the entrapment and loading of drugs in the matrix of NLC. A preliminary investigation was done with a wide variety of solid-to-liquid lipid ratios and surfactant concentrations. The ratio of solid to liquid lipids was varied from 70:30 to 80:20, and the percentage concentration of surfactant was varied from 1-1.5%. As the drug is water soluble (13.4 mg/ml at 25°C), the critical points considered were the effect of composition on the drug entrapment and drug loading[14].

#### 4.3. Employment of design

The 'I optimal' design (Design Expert software V11) was used to create the formulations, with the percentage of drug entrapment, the percentage of drug loading, and the particle size of the nanocarriers serving as the dependent variables. The independent factors used in the design were the concentration of surfactant and the ratio of solid and liquid lipids at two levels. The I-optimal design is used to minimize the variations in the average prediction over the design space to avoid bias and brings precision in the estimation of the effect of independent variables over the dependent ones. The design yielded 14 trials with a minimum variance of the independent variables within their levels (**Hata! Başyuru kaynağı bulunamadı.**). Experimentations were planned for the 14 runs to maximize the composition effects on drug entrapment and loading.

Table 6. Design of Experiment

Formulation code	SL: LL	Conc. of surfactant
F1	-1	-0.69
F2	-0.13	0.15
F3	-0.12	1
F4	-1	0.152
F5	-1	1
F7	0.257	-1
F8	1	-1
F9	-1	-0.69
F10	-0.13	0.15
F11	0.74	1
F12	-0.3	0.15
F13	0.581	0.293
F14	1	-0.3

#### 4.4. Preparation of NLCs of TDF

Nano lipid carriers were prepared using high shear homogenization method. A quantity of 200 mg TDF was included in the formulations containing 800 mg of total lipids. Poloxamer 188 solution (1.5%w/v) was prepared with water. Stearic acid and oleic acid were dissolved in acetone. The drug was dissolved in poloxamer 188 solution. The lipid mixture was subjected to homogenization at 5000 rpm for 15 min with the dropwise addition of drug solution to get an emulsion. The formed emulsion was poured on a chilled petridish and kept at ambient temperature until it was completely cooled to form nano lipid carriers[14].

#### 4.5. Evaluation of NLC of TDF

##### 4.5.1. Estimation of percentage drug entrapment and drug loading

The total drug content of the formulations was determined by dispersing a known quantity of each formulation in methanol. An aliquot of the dispersion was filtered using a 0.22 µm syringe filter and diluted with 1:1 ratio of phosphate buffer (pH 2.5) and acetonitrile, and absorbance was noted at 250 nm in a UV-Vis spectrophotometer. The process was repeated thrice to estimate the total drug content. To determine the free



drug a known quantity of sample was dispersed in phosphate buffer (pH 2.5), centrifuged at 5000 rpm for 10 min, the supernatant was collected and diluted suitable with a 1:1 ratio of phosphate buffer (pH 2.5), and acetonitrile and free drug was estimated. An average of three trials were taken for the estimation[15]. The formula to calculate entrapment efficiency was as follows,

$$\% \text{Entrapment Efficiency} = \frac{\text{Total drug-free drug}}{\text{Total drug}} \times 100$$

Drug loading was calculated using the formula [16]

$$\% \text{Drug loading} = \frac{\text{Total drug}}{\text{yield}} \times 100$$

#### 4.5.2. Estimation of particle size and zeta potential

The zeta potential and particle size of the formulations were estimated using Horiba, SZ 100, Japan. The dynamic light scattering principle was used. The formulation was dispersed in milli-pore water and was ultrasonicated for 10 min. Measurement was made in triplicate at 90 ° and 25 °C [17].

#### 4.5.3. Fourier Transform Infrared (FTIR) Spectroscopy

At 25.0 ± 0.5 °C Bruker ATR alpha method was used to create the spectra of the pure drug, blank optimized NLC, and TDF-loaded NLC in the region of 4000-400 cm<sup>-1</sup>[18].

#### 4.5.4. Scanning Electron Microscopy (SEM)

SEM images of the nanoparticles were taken. Gold was sputtered on the optimized TDF formulation, which was then vacuum dried and examined with an SEM (JSM-7500F, JEOL Ltd., Japan) operating at an acceleration voltage of 10.0 kV[19].

#### 4.5.5. In-vitro drug release study for nano lipid carriers

The Franz diffusion cell device was used for *in-vitro* drug release research. A sample corresponding to 40 mg TDF was put into the Franz diffusion cell system, and the junction between the donor and receptor compartments was sealed with a 14000 KD dialysis membrane (Hi media, that had been soaked overnight in phosphate buffer 6.8). The optimized formulation was dispersed in 2.5 ml of phosphate buffer pH 6.8 in the donor compartment, and 40 ml of phosphate buffer pH 6.8 was present in the receptor compartment. The temperature was kept at 37 °C while being stirred continuously at 50 rpm. At predetermined hourly intervals of up to 8 hours, aliquots of the samples were collected, and the same volume was replenished with fresh buffer. Spectrophotometric analysis was used to determine the amount of medication emitted[20]. The same process was followed for the evaluation of nano lipid carrier loaded oro mucosal film of TDF at the later stage.

### 4.6. Preparations of NLC loaded oro-mucoadhesive films

By solvent casting, nano lipid carrier loaded oro mucosal adhesive films were prepared using a 3:2 polymer mix of HPMC and Carbopol 934. The polymers were dispersed in the solvent system of isopropyl alcohol and dichloromethane (1:2 ratio) with propylene glycol (0.4% v/v) as a plasticizer for 5 h with continuous stirring. Required quantities of NLC were added and stirring was continued till the NLC gets dispersed completely. The film was cast on a fabricated glass mold of 4 cm<sup>2</sup> and allowed to dry in the oven for 50-60 min[21]. TDF was reported to be thermostable, as reported by Havele S *et al*[22].

### 4.7. Evaluation of NLC loaded oro-mucosal adhesive film

#### 4.7.1. Muco-adhesion property

Test for adhesion was performed to check the residence time of the film in the oral cavity after its administration. A small piece of film (4 cm<sup>2</sup>) was taken in a petri-plate and 2-3 ml of phosphate buffer of pH 6.8 was added. Allow it to rest till the film dissolves completely in the phosphate buffer. The duration till the film completely dissolves was noted[3].

#### 4.7.2. Mechanical properties of the film

Using vernier calipers the thickness of the film was measured. The film (4 cm<sup>2</sup>) was placed between the vernier calipers and measured for thickness. The study was performed in triplicate [23]. The folding endurance of the films was tested by repeatedly folding the center portion of the films until they tore [24].

#### 4.7.3. Surface pH test

The muco-adhesive films were allowed in contact with distilled water. The surface pH was estimated with a digital pH meter.

#### 4.7.4. Swelling test

The swelling test for the film (4 cm<sup>2</sup>) was performed using phosphate buffer solution pH.6.8 Film sample was weighed and put in a small jar with 2–3 ml of PBS. The weight of the film was measured after 24 h [25].

$$\text{Swelling index} = \frac{W_2 - W_1}{W_2} \times 100$$

#### 4.7.5. Estimation of drug content

Drug content was determined by dissolving a piece of film (4 cm<sup>2</sup>) in methanol. The solution was subjected to vortex for 10–15 min. Then aliquot of the sample was diluted suitably and estimated spectrophotometrically. The sample was observed for absorbance in UV spectrophotometer using distilled water as blank. Trials were performed in triplicate [26–27]. The drug content in the film was calculated as follows,

$$\% \text{Drug content} = \frac{\text{Actual amount of drug in film} \times 100}{\text{Theoretical amount of drug in the film}}$$

#### 4.7.6. Differential Scanning Calorimetry (DSC)

Perkin-Elmer 4000 series instruments were used to characterize the physical state of the pure drug, optimized NLC, and NLC-loaded film of TDF. Samples were placed in aluminum pans and were heated at an increment of 10 °C per minute under nitrogen atmosphere between 40 °C and 400 °C [28].

#### 4.7.8. Ex-vivo permeation study

In a Franz diffusion cell, the *ex vivo* permeation of an NLC-loaded TDF film was performed over goat buccal mucosa using phosphate buffer pH 6.8 as the medium. Goat buccal mucosa was procured from a local abattoir and stored in phosphate buffer pH 6.8 after cleaning with isotonic phosphate buffer. Buccal mucosa was placed between the donor and receptor compartments, on which the strip of the NLC-loaded film (4 cm<sup>2</sup>) was placed. A temperature of 37 °C and 50 rpm magnetic stirring of the assembly was maintained throughout the research. At predetermined intervals, a specific volume of aliquots was removed and replaced with a similar volume of the new medium. After appropriate dilution, the extracted samples were examined for TDF content using a UV spectrophotometer at 250 nm [29].

**Acknowledgment:** We the authors are highly grateful to the Principal and Management of Krupanidhi College of Pharmacy, Bangalore for providing the facility to conduct the study. We are thankful to Viatrix Hyderabad for their generous support of the gift sample of the drug.

**Author contributions:** Concept – S.B. K.H.K; Design – S.B. K.H.K; Supervision – S.B.; Resources – S.B. K.H.K; Materials – S.B. K.H.K; Data Collection and/or Processing – S.B. K.H.K; Analysis and/or Interpretation S.B. K.H.K.; Literature Search – S.B. K.H.K; Writing – S.B. K.H.K.; Critical Reviews – S.B. K.H.K.

**Conflict of interest statement:** The authors declared no conflict of interest in the manuscript.

## REFERENCES

- [1] Ray AS, Fordyce MW, Hitchcock MJM. Tenofovir alafenamide: A novel prodrug of tenofovir for the treatment of human immunodeficiency virus. *Antiviral Res.* 2016;125:63–70. <https://doi.org/10.1016/j.antiviral.2015.11.009>
- [2] Chauhan I, Yasir M, Verma M, Singh AP. Nanostructured lipid carriers: A groundbreaking approach for transdermal drug delivery. *Adv Pharm Bull.* 2020;10(2):150–165. <https://doi.org/10.34172/apb.2020.021>

- [3] Basahih TS, Alamoudi AA, El-Say KM, Alhakamy NA, Ahmed OAA. Improved transmucosal delivery of glimepiride via unidirectional release buccal film loaded with vitamin e tpgs-based nanocarrier. *Dose-Response*. 2020;18(3):1559325820945164. <https://doi.org/10.1177/1559325820945164>
- [4] Haider M, Abdin SM, Kamal L, Orive G. Nanostructured lipid carriers for delivery of chemotherapeutics: A review. *Pharmaceutics*. 2020;12(3):1–26. <https://doi.org/10.3390/pharmaceutics12030288>
- [5] Reddy HV R, Bhattacharyya S. Mucoadhesive buccal delivery of drugs- challenges and present aspects. *Indian drugs*. 2020;57(6):7-20. <https://doi.org/10.53879/id.57.06.12294>
- [6] Reddy HV R, Bhattacharyya S. In vitro evaluation of mucoadhesive in situ nanogel of celecoxib for buccal delivery. *Ann Pharm Fr*. 2021;79(4):418–430. <https://doi.org/10.1016/j.pharma.2021.01.006>
- [7] Alopaeus JF, Hellfritzsch M, Gutowski T, Scherließ R, Almeida A, Sarmento B, Natasa SB, Tho I. Mucoadhesive buccal films based on a graft co-polymer – A mucin-retentive hydrogel scaffold. *Eur J Pharm Sci*. 2020;142:105142. <https://doi.org/10.1016/j.ejps.2019.105142>
- [8] Tenofovir disoproxil: uses, interactions, mechanism of action | DrugBank Online. <https://doi.org/10.1016/j.ejps.2019.105142>
- [9] Khan AB, Thakur RS. Formulation and evaluation of mucoadhesive microspheres of tenofovir disoproxil fumarate for intravaginal use. *Curr Drug Del*. 2014;11(1):112-122. <https://doi.org/10.2174/156720181000131028120709>
- [10] Patel D, Dasgupta S, Dey S, Ramani YR, Ray S, Mazumder B. Nanostructured Lipid Carriers (NLC)-based gel for the topical delivery of aceclofenac: Preparation, characterization, and in vivo evaluation. *Sci Pharm*. 2012;80(3):749-764. <http://dx.doi.org/10.3797/scipharm.1202-12>
- [11] Alhayali A, Rao PV, Velaga S. Silodosin oral films: Development, physico-mechanical properties and *in vitro* dissolution studies in simulated saliva. *J Drug Del Sci Tech*. 2019;53:101122. <https://doi.org/10.1016/j.jddst.2019.06.019>
- [12] Dhawale P, Mahajan NM, Mahapatra DK, Mahajan UN, Gangane PS. HPMC K15M and Carbopol 940 mediated fabrication of ondansetron hydrochloride intranasal mucoadhesive microspheres. *J Appl Pharm Sci*. 2018;8(08): 075-083. <https://doi.org/10.7324/JAPS.2018.8812>
- [13] Kovačević AB, Müller RH, Keck CM. Formulation development of lipid nanoparticles: Improved lipid screening and development of tacrolimus loaded nanostructured lipid carriers (NLC). *Int J Pharm*. 2020;576:118918. <https://doi.org/10.1016/j.ijpharm.2019.118918>
- [14] Jafarifar Z, Rezaie M, Sharifan P, Jahani V, Daneshmand S, Ghazizadeh H, Ferns GA, Shiva G, Majid GM. Preparation and characterization of nanostructured lipid carrier (NLC) and nanoemulsion containing vitamin d3. *Appl Biochem Biotechnol*. 2022;194(2):914–929. <https://doi.org/10.1007/s12010-021-03656-z>
- [15] Harshitha C, Bhattacharyya S. Statistical optimization amalgamated approach on formulation development of nano lipid carrier loaded hydrophilic gel of fluticasone propionate. *Indian J Pharm Edu Res*. 2021;55(2):1-10. <https://doi.org/10.5530/ijper.55.2.79>
- [16] Liu D, Liu Z, Wang L, Zhang C, Zhang N. Nanostructured lipid carriers as novel carrier for parenteral delivery of docetaxel. *Colloids and Surf B: Biointerfaces*. 2011;85(2):262–269. <https://doi.org/10.1016/j.colsurfb.2011.02.038>
- [17] Yaghoubi A, Ghojzadeh M, Abolhasani S, Alikhah H, Khaki-Khatibi F. Correlation of serum levels of vitronectin, malondialdehyde and hs-crp with disease severity in coronary artery disease. *J Cardiovasc Thorac Res*. 2015;7(3):113–117. <https://doi.org/10.15171%2Fjcvtr.2015.24>
- [18] Guilherme VA, Ribeiro LNM, Alcântara ACS, Castro SR, Rodrigues da Silva GH, da Silva CG, Marcia CB, Juliana CN, Dristina GM, Abdalla HB, Bonfante R, Cereda CMS, Paula ED. Improved efficacy of naproxen-loaded NLC for temporomandibular joint administration. *Sci Rep*. 2019;9(1):1–11. <https://doi.org/10.1038/s41598-019-47486-w>
- [19] Pi J, Wang S, Li W, Kebebe D, Zhang Y, Zhang B, Qi D, Guo P, Li N, Liu Z. A nano-cocrystal strategy to improve the dissolution rate and oral bioavailability of baicalein. *Asian J Pharm Sci*. 2019; 14:154–164. <https://doi.org/10.1016/j.ajps.2018.04.009>
- [20] Takeuchi K, Watanabe M, Yanagi M, Murakami I, Hosono H, Nishizawa S, Chigono Y, Hirabayashi S, Matsuda J, Yamaoka K, Inoue K. In vitro and clinical evaluation of an oral mucosal adhesive film containing indomethacin. *Yakugaku Zasshi*. 2008;128(12):1791–1795. <https://doi.org/10.1248/yakushi.128.1791>
- [21] Bhattacharyya S, RangaRao BG. Formulation and development of oral disintegrating film of fexofenadine hydrochloride. *Acta Pharm Sci*. 2022;60 (4):345–362. <https://doi.org/10.23893/1307-2080.APS6023>

- [22] Havele S, Dhaneshwar S. Stress studies of tenofovir disoproxil fumarate by HPTLC in bulk drug and pharmaceutical formulation. *Sci World J*. 2012;894136. <https://doi.org/10.1100/2012/894136>
- [23] Mahajan HS, Deshmukh SR. Development and evaluation of gel-forming ocular films based on xyloglucan. *Carbohydr Polym*. 2015;122:243–247. <https://doi.org/10.1016/j.carbpol>
- [24] Preis M, Woertz C, Kleinebudde P, Breitzkreutz J. Oromucosal film preparations: Classification and characterization methods. *Expert Opin Drug Deliv*. 2013;10(9):1303–1317. <https://doi.org/10.1517/17425247.2013.804058>
- [25] Mahboob MBH, Riaz T, Jamshaid M, Bashir I, Zulfiqar S. Oral films: A comprehensive review. *Int Cur Pharm J*. 2016;5(12):111–117. <https://doi.org/10.3329/icpj.v5i12.30413>
- [26] Satishbabu B, Srinivasan B. Preparation and evaluation of buccoadhesive films of atenolol. *Indian J Pharm Sci*. 2008;70(2):175–179. <https://doi.org/10.4103%2F0250-474X.41451>.
- [27] Jovanović M, Tomić N, Cvijić S, Stojanović D, Ibrić S, Uskoković P. Mucoadhesive gelatin buccal films with propranolol hydrochloride: Evaluation of mechanical, mucoadhesive, and biopharmaceutical properties. *Pharmaceutics*. 2021;13(2):1–19. <https://doi.org/10.3390/pharmaceutics13020273>
- [28] Gaba B, Fazil M, Khan S, Ali A, Baboota S, Ali J. Nanostructured lipid carrier system for topical delivery of terbinafine hydrochloride. *Bull Fac Pharm*. 2015;53(2):147–159. <https://doi.org/10.1016/j.bfopcu.2015.10.001>
- [29] Kamble RN, Mehtre R V., Mehta PP, Nangare P, Patil SS. Albendazole electrospun nanofiber films: in-vitro and ex-vivo assessment. *Bionanoscience*. 2019;9(3):625–636. <https://doi.org/10.1007/s12668-019-00627-x>